Cement-Based Piezoelectric Ceramic Composites

Subjects: Materials Science, Composites | Engineering, Civil
Contributor: Yuqing Liu

Compatibility, a critical issue between sensing material and host structure, significantly influences the detecting performance (e.g., sensitive, signal-to-noise ratio) of the embedded sensor. To address this issue in concrete-based infrastructural health monitoring, cement-based piezoelectric composites (piezoelectric ceramic particles as a function phase and cementitious materials as a matrix) have attracted continuous attention in the past two decades, dramatically exhibiting superior durability, sensitivity, and compatibility.

Keywords: sensing element ; piezoelectric ceramic composite ; fabrication ; properties ; structural health monitoring

1. Introduction

Infrastructure, a series of fundamental facilities and structure systems, performs indispensable support for society, expected to achieve sustainability and economic efficiency. However, safety hazards caused by progressive deterioration with age [1] and serious disasters related to severe environmental conditions (freeze–thaw cycles [2][3], marine environment [4], high temperature [5], etc.) are the potential issues during the lifespan of infrastructure, possibly leading to a shortened service life and high maintenance/reconstruction costs. Concrete, regarded as an affordable, durable, and dramatic building material, has been widely applied in infrastructure [6][7][8][9][10]. Due to the adverse impact of intrinsic (material self-defects [11], deficient structural design and construction, etc.) and extrinsic (severe environment, accidental loading [12], etc.) factors, concrete structures usually undergo deterioration during the whole lifespan, such as concrete cracking [13], steel corrosion [14][15], spalling [16], and structure collapse [17].

Most serious durability and safety issues for concrete-based infrastructure are usually the cumulative consequence induced by the service environment [18][19], aging [20], and self-defects [21]. At different periods of its lifespan, there are various dominant factors for degeneration. In the concreting process, fresh concrete can be easily influenced by temperature, humidity, and rheological properties, possibly leading to self-defects (cracks and pores). During the service life, aggressive action related to the invasive substances (chloride, carbon dioxide, and sulfate, etc.) and environmental change is the major reason for the deterioration (e.g., corrosion, carbonation, and cracking). As concrete structures age, the deterioration will decrease the ultimate load capacity and further bring safety and serviceability risks. The application of eco-friendly materials (e.g., recycled concrete [22] and aggregate [10], seawater [23] and sea sand [24], and geopolymer [25][26]) in construction is another challenge for the structural performance. Due to durability and safety issues, concrete-based infrastructure will struggle to maintain functionality, and the most affordable solution (e.g., repair, upgrade, and partial reconstruction) needs to be filtrated.

Considering the severe consequences caused by structural deterioration, there is a strong demand for implementing identification strategies and protection for concrete-based infrastructure. An innovative, reliable, and cost-effective structural health monitoring (SHM) technique for constructing/existing infrastructure has been an essential item to diagnose and mitigate damages and further ensure its functionality, thereby elongating the service life. The strategy of efficient and accurate SHM systems with intelligent materials (e.g., optical fiber [27], piezoelectric materials [28]) installed in concrete structures has attracted lots of attention in recent decades [29][30][31][32]. Piezoelectric materials can be encapsulated as smart aggregates and embedded into the concrete structure, thereby monitoring the deterioration process. The distinction in acoustic impedance, density, and mechanics properties leads to the lower compatibility between the sensing element and host structures, resulting in signal capture disturbance. Table 1 summarizes the major parameters that lead to the incompatibility among cement, concrete and piezoelectric ceramics. One of the critical factors for signal acquisition is acoustic impedance, determined by the density and acoustic velocity [33]. The acoustic velocities of piezoelectric ceramic, cement, and plain concrete are similar, while the density of piezoelectric ceramic is much higher, resulting in the acoustic impedance mismatching problem. The piezoelectric composite is an alternative approach to address this issue. In 2002, cement-based piezoelectric composites (CPCs), innovated by Li et al. [34], are regarded as a pioneering inorganic piezoelectric composite, more adaptable to the concrete structure. Based on the connectivity, piezoelectric composite materials can be divided into 10 basic types [35]. The superiority of the 0-3/1-3/2-2 type CPCs applied in SHM has been demonstrated. The 1-3 [36]/2-2 [37] types can be regarded as the development based on 0-3 by controlling the distribution of piezoelectric materials in the cement matrix. Despite the lower piezoelectric strain constant (d_{33}), 0-3 CPCs show an excellent overall performance (e.g., higher piezoelectric voltage constant (g_{33}), acoustic impedance matching, and flexibility) as a better alternative material for sensing elements, and also show a prospect in combining intelligent manufacturing. However, the difference in fabrication parameters and various raw materials sources leads to a great variety in the final piezoelectric performance.

Table 1. Physical properties of piezoelectric ceramic, cement paste and concrete.

Items	Materials		
	Piezoelectric Ceramic	Cement Paste	Plain Concrete
Density (10^3 kg/m^3)	**4.64–7.6** [33][38][39]	**2.0–2.2** [37]	**2.4** [40]
Acoustic velocity (10^3 m/s)	**2.83–3.40** [40]	**2.64–3.37** [37][40]	**3.0–4.2** [37][40]
Acoustic impedance (MRayl)	**21.2–30** [37]	**3.5–8** [41]	**6.9–10.4** [42]
Elasticity modulus (GPa)	**50–75** [38][43]	**10–20** [44]	**19.0–48.6** [45]

In the last two decades, the performance improvement of CPCs has been performed. The significant variety in the final piezoelectric performance illustrates the existing shortcoming and insufficient understanding around the composite. Our main objective in this review is to recapitulate the previous studies related to CPCs and discuss the influence of raw materials and the main problems in fabrication, thereby promoting advanced piezoelectric composite design, fabrication, and application. Moreover, the present review will summarize previous research to sort out the critical influencing factors and potential directions. Then, to clarify the influencing factors of the composite materials, theories and fundamentals, experimental and modeling analysis, raw materials, the fabrication process, and application are presented in different sections. At the end of each section, insightful viewpoints and prospective studies on the composite will be provided.

2. Recent Study on Cement-Based Piezoelectric Composites

The piezoelectric performance (e.g., piezoelectric, electromechanical coupling, and dielectric properties) of CPCs has been comprehensively characterized and discussed. Initially, Li et al. [30] reported the feasibility of CPCs and characterized their performance, including the piezoelectric strain factor (d_{33}), piezoelectric voltage factor (g_{33}), electromechanical coupling coefficient (K_t and K_p), and dielectric constant (ε_r). Subsequently, Huang et al. [46] studied the polarization process of PZT/sulphoaluminate cement composites; Chaipanich et al. [47] demonstrated the properties of PZT–ordinary Portland cement composites. These studies have demonstrated the feasibility of CPCs and revealed that the piezoelectric particles' higher content could improve the piezoelectric performance. Additionally, Chaipanich et al. [48] studied the particle size effect, showing that a larger particle of the function phase is beneficial for improving the d_{33} and ε_r. Pan et al. [49] and Chomyen et al. [50] demonstrated improved piezoelectric performance by adding fly ash, respectively. However, the final piezoelectric performance shows a tremendous difference, mainly attributed to the difference in piezoelectric materials and polarization parameters. According to the above researches, the main influencing factors on the all-round performance can be summarized as the (a) matrix; (b) functional phase (piezoelectric materials); (c) fabrication process; (d) aging.

Due to the complex hydration product composition and heterogeneous microstructure, the matrix effect on piezoelectric performance has been investigated. Among these, enhancing d_{33} is still the primary target. The low-efficiency stress transfer between matrix and piezoelectric particles caused by the poor connectivity and porosity is the main reason for the lower d_{33}. Therefore, a denser matrix is a penitential approach to optimize it. Chaipanich et al. [51] revealed that the d_{33} shows a slight increase with adding silica fume. Wang et al. [52] found that adding silica-based material can improve the d_{33} even up to 99.0 pC/N due to the ITZ optimization under the conditions of compression forming, steam curing, and aging. Subsequently, to decrease porosities, slag, fly ash, and kaolin was studied by Pan et al. [49][53], tracing the piezoelectric properties in different ages, and the highest d_{33} can reach 111.1 pC/N. Wittinanon et al. [38] employed PVDF to modify the ITZ and reduce the porosity, showing a significant optimization in reducing leakage current. Considering the positive effect of the higher matrix conductivity during the polarization process, carbon materials (carbon addition [54], carbon black [55][56], carbon nanotube [57], and graphene nanoplatelets [58]) were also applied to optimize the piezoelectric properties. The matrix properties can also affect the g_{33}, K_t, K_p, ε_r, and dielectric loss (*tan δ*), and the increase of parameter values (K_t, ε_r, and g_{33}) with the help of admixture has been reported [49][55]. The output voltage (V) of the composite mixed with basalt fiber, which affects the matrix's elastic modulus, was also characterized [43].

Meanwhile, the fabrication process optimization was also carried out, and some steps demonstrate significant improvement. Huang et al. [59] applied the forming pressure to fabricate the CPCs, which could help obtain a denser matrix and further enhance the d_{33}. Furthermore, the curing is also essential to obtain the higher piezoelectric performance because inadequate curing would cause interfacial cracks and lead to a locally poor value of d_{33}. Considering the positive effect of the high temperature on the hydration evaluation, Wang et al. [52] carried out the hot water and steam curing process, respectively. Pan et al. [60] found that the pre-heating treatment could improve the polarization efficiency due to decreased moisture. The above fabrication process development could contribute to a better microstructure and mitigate the negative effect caused by the ITZ between the cement matrix and piezoelectric ceramic particles. The significance of polarization has been studied by Huang et al. [46] and Dong et al. [61], demonstrating that the voltage, polarization time, and temperature can directly play a decisive role.

Recently, the multi-factors coupling for the design and fabrication of the composite has been considered. Among those factors, aging is the key influential factor combined with the materials and fabrication process for the performance of CPCs. Dong et al. [37] and Huang et al. [62] revealed the d_{33} increase with time, even though the matrix phase in their studies is different. Later, Chaipanich et al. [63] found the increased trend of d_{33} in PZT-Portland cement composites with time; Pan et al. [53] also characterized this phenomenon during their investigation into the effect of admixture. In 2016, Pan et al. [60] found that heat treatment could improve the comprehensive performance after aging. Subsequently, the effect of the water/cement ratio and time on the piezoelectric performance was also studied [64].

The application of this composite has been carried out. Lu et al. [29][30][40][65] systemically monitored the different states in concrete using embedded CPCs sensors, including hydration, crack, and corrosion. Xing et al. [66] tested the electrical response of this material under different mechanical loadings. Pan et al. [31] applied the composite for monitoring the strength growth of concrete via electromechanical impedance. Those applications reveal the feasibility and superiority of CPCs as a potential sensing element.

Regarding the environmental issues, lead-free piezoelectric material has attracted increasing attention. Rianyoi et al. [38][67][68][69] prepared the barium titanate-cement composites and characterized the influence of the particle size and polyvinylidene fluoride (PVDF). Chaipanich et al. [39][50][70][71][72][73] fabricated barium zirconate titanate-cement composites and studied their microstructure and piezoelectric performance. Hunpratub et al. [74] believe that BCTZO ($Ba_{0.85}Ca_{0.15}Ti_{0.9}Zr_{0.1}O_3$) particle is an alternative material as function phase and revealed the effect of particle size on dielectric and piezoelectric properties. Additionally, BNBT ($0.94(Bi_{0.5}Na_{0.5})TiO_3$-$0.06BaTiO_3$) [75] and BNBK ($0.88Bi_{0.5}Na_{0.5}TiO_3$-$0.08Bi_{0.5}K_{0.5}TiO_3$-$0.04BaTiO_3$) [76] have been used as a function phase to fabricate the composite. Although lead-free piezoelectric materials are potential functional materials, the lower piezoelectric properties and poor temperature stability still limit their application in CPCs.

Numerous studies have illustrated the feasibility to fabricate and employ this composite as a sensing element. However, the effect of the fabrication process and polarization parameters are still essential to further study due to the physical and chemical distinction between cementitious materials and piezoelectric materials. The properties of lead-based/lead-free piezoelectric ceramic and its cement-based composites in recent studies, including d_{33}, g_{33}, ε_r, K_t, and acoustic impedance, are intuitively summarized in Table 2. The highest value of d_{33} in lead-free CPCs is 61.5 pC/N, while that of lead-bearing CPCs is 87 pC/N initially. However, the d_{33} of the lead-bearing composite can reach over 140 pC/N after aging, close to the piezoelectric ceramic. It should be mentioned that these higher parameters almost attribute to the positive effect of aging, and the typical studies for tracing the change of d_{33} with aging are illustrated in Figure 1. Only a few studies can obtain high piezoelectric performance at the initial stage after polarization. Santos et al. [77] reported that the curing process of CPCs has a direct relationship with its dielectric properties and electrical conductivity, attributing to the existence of unstable dipoles, which would be a suitable example for understanding the performance variation, illustrating the significant effect of the matrix properties on the final performance. Kantakam et al. [78] revealed the tremendous influence of the matrix material on the dielectric properties.

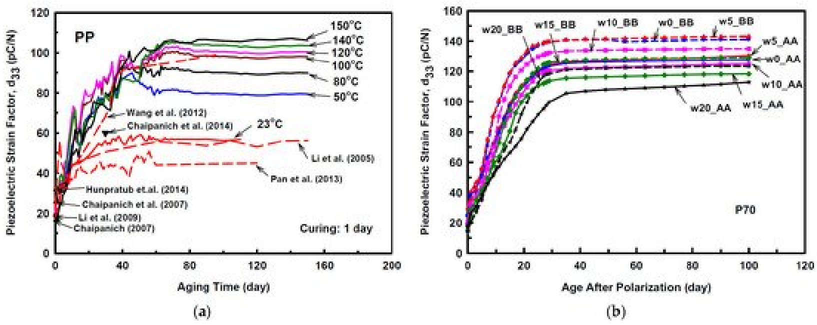

Figure 1. (**a**) Piezoelectric strain constant of cement piezoelectric composites. Reprinted with permission from ref. [79]. Copyright 2016 Elsevier. (**b**) Piezoelectric strain factor of 70% PZT/cement composites versus age. Reprinted with permission from ref. [64]. Copyright 2013 Elsevier.

Table 2. Piezoelectric properties of piezoelectric materials.

Items	Piezoelectric Materials			
	Lead-Based Piezoelectric Ceramic	Lead-Free Piezoelectric Ceramic	Lead-Bearing CPCs	Lead-Free CPCs
Piezoelectric strain factor d_{33} (10^{-12} C/N)	215~513 [80]	190~235 [38][39]	0.5~87 [45][81] 5 *~143 * [37][52][64]	4~61.5 [74][75]
Piezoelectric voltage factor g_{33} (10^{-3} Vm/N)	15.9~25 [80]	12.43~18.28 [38][39]	15~60 [34][82][83] 20 *~30 * [79]	7~33.59 [38][75]
Dielectric constant ε_r (at 1 kHz)	1050~3643 [37][77]	1452~1726 [38][39]	43.5~536 [34][47][48] 1017.6~1834.2 [78] 280 *~890 * [60][64]	120~350 [38][39]
Thickness electromechanical coupling coefficient K_t (%)	40~67 [80]	-	9.47~28.19 [34][80] 13.16 *~13.53 * [53][60]	9~14 [67]
Acoustic impedance Z (10^6 kg/m^2 s)	21.2~36 [33][37]	25.2~34 [33][38]	~9.6 [32]	7.5~10.5 [67][70][75]

References

1. Chen, S.; Lu, L.; Xiang, Y.; Lu, Q.; Li, M. A data heterogeneity modeling and quantification approach for field pre-assessment of chloride-induced corrosion in aging infrastructures. Reliab. Eng. Syst. Saf. 2018, 171, 123–135.
2. Smith, S.H.; Qiao, C.; Suraneni, P.; Kurtis, K.E.; Weiss, W.J. Service-life of concrete in freeze-thaw environments: Critical degree of saturation and calcium oxychloride formation. Cem. Concr. Res. 2019, 122, 93–106.
3. Teng, F.; Qiu, W.-L.; Pan, S.-S.; Hu, H.-S. Experimental study on seismic performance of precast segmental concrete columns after seawater freeze-thaw cycles. Constr. Build. Mater. 2020, 260, 120482.
4. Qu, F.; Li, W.; Dong, W.; Tam, V.W.; Yu, T. Durability deterioration of concrete under marine environment from material to structure: A critical review. J. Build. Eng. 2021, 35, 102074.
5. Zeiml, M.; Lackner, R.; Leithner, D.; Eberhardsteiner, J. Identification of residual gas-transport properties of concrete subjected to high temperatures. Cem. Concr. Res. 2008, 38, 699–716.
6. Talukdar, S.N.; Banthia, N.; Grace, J.R. Carbonation in concrete infrastructure in the context of global climate change—Part 1: Experimental results and model development. Cem. Concr. Compos. 2012, 34, 924–930.
7. Arabzadeh, A.; Notani, M.A.; Zadeh, A.K.; Nahvi, A.; Sassani, A.; Ceylan, H. Electrically conductive asphalt concrete: An alternative for automating the winter maintenance operations of transportation infrastructure. Compos. Eng. 2019, 173, 106985.
8. Guo, P.; Meng, W.; Nassif, H.; Gou, H.; Bao, Y. New perspectives on recycling waste glass in manufacturing concrete for sustainable civil infrastructure. Constr. Build. Mater. 2020, 257, 119579.
9. Han, N. Role of NDE in quality control during construction of concrete infrastructures on the basis of service life design. Constr. Build. Mater. 2004, 18, 163–172.
10. Surya, M.; Vvl, K.R.; Lakshmy, P. Recycled Aggregate Concrete for Transportation Infrastructure. Procedia Soc. Behav. Sci. 2013, 104, 1158–1167.
11. Mehta, P.K.; Monteiro, P.J.M. Concrete: Microstructure, Properties, and Materials; Prentice-Hall: Hoboken, NJ, USA, 2013.
12. Lin, F.; Li, Y.; Gu, X.; Zhao, X.; Tang, D. Prediction of ground vibration due to the collapse of a 235 m high cooling tower under accidental loads. Nucl. Eng. Des. 2013, 258, 89–101.
13. Fang, G.; Liu, Y.; Qin, S.; Ding, W.; Zhang, J.; Hong, S.; Xing, F.; Dong, B. Visualized tracing of crack self-healing features in cement/microcapsule system with X-ray microcomputed tomography. Constr. Build. Mater. 2018, 179, 336–347.

14. Dong, B.; Ding, W.; Qin, S.; Han, N.; Fang, G.; Liu, Y.; Xing, F.; Hong, S. Chemical self-healing system with novel microcapsules for corrosion inhibition of rebar in concrete. Cem. Concr. Compos. 2018, 85, 83–91.

15. Dong, B.; Ding, W.; Qin, S.; Fang, G.; Liu, Y.; Dong, P.; Han, S.; Xing, F.; Hong, S. 3D visualized tracing of rebar corrosion-inhibiting features in concrete with a novel chemical self-healing system. Constr. Build. Mater. 2018, 168, 11–20.

16. Barnes, R. Corrosion of Steel in Concrete—Understanding, Investigation and Repair, 2nd ed.; John Wiley & Sons, Inc.: Hoboken, NJ, USA, 2006.

17. Zhou, Y.; Hu, X.; Pei, Y.; Hwang, H.-J.; Chen, T.; Yi, W.; Deng, L. Dynamic load test on progressive collapse resistance of fully assembled precast concrete frame structures. Eng. Struct. 2020, 214, 110675.

18. Hussain, S.; Bhunia, D.; Singh, S. Comparative study of accelerated carbonation of plain cement and fly-ash concrete. J. Build. Eng. 2017, 10, 26–31.

19. Tang, S.; Yao, Y.; Andrade, C.; Li, Z. Recent durability studies on concrete structure. Cem. Concr. Res. 2015, 78, 143–154.

20. Farshad, H.; Mahdi, Y. The probabilistic seismic assessment of aged concrete arch bridges: The role of soil-structure interaction. Structures 2020, 28, 894–904.

21. Xin, J.; Zhang, G.; Liu, Y.; Wang, Z.; Wu, Z. Evaluation of behavior and cracking potential of early-age cementitious systems using uniaxial restraint tests: A review. Constr. Build. Mater. 2020, 231, 117146.

22. Han, Y.; Yang, Z.; Ding, T.; Xiao, J. Environmental and economic assessment on 3D printed buildings with recycled concrete. J. Clean. Prod. 2021, 278, 123884.

23. Li, P.; Li, W.; Yu, T.; Qu, F.; Tam, V.W. Investigation on early-age hydration, mechanical properties and microstructure of seawater sea sand cement mortar. Constr. Build. Mater. 2020, 249, 118776.

24. Guo, M.; Hu, B.; Xing, F.; Zhou, X.; Sun, M.; Sui, L.; Zhou, Y. Characterization of the mechanical properties of eco-friendly concrete made with untreated sea sand and seawater based on statistical analysis. Constr. Build. Mater. 2020, 234, 117339.

25. Wang, Y.-S.; Alrefaei, Y.; Dai, J.-G. Influence of coal fly ash on the early performance enhancement and formation mechanisms of silico-aluminophosphate geopolymer. Cem. Concr. Res. 2020, 127, 105932.

26. Panda, B.; Unluer, C.; Tan, M.J. Investigation of the rheology and strength of geopolymer mixtures for extrusion-based 3D printing. Cem. Concr. Compos. 2018, 94, 307–314.

27. Mata-Falcón, J.; Haefliger, S.; Lee, M.; Galkovski, T.; Gehri, N. Combined application of distributed fibre optical and digital image correlation measurements to structural concrete experiments. Eng. Struct. 2020, 225, 111309.

28. Tuloup, C.; Harizi, W.; Aboura, Z.; Meyer, Y.; Khellil, K.; Lachat, R. On the use of in-situ piezoelectric sensors for the manufacturing and structural health monitoring of polymer-matrix composites: A literature review. Compos. Struct. 2019, 215, 127–149.

29. Lu, Y.; Li, Z.; Qin, L. Signal-based acoustic emission monitoring on mortar using cement-based piezoelectric sensors. ACI Mater. J. 2011, 108, 178–186.

30. Lu, Y.; Zhang, J.; Li, Z. Study on hydration process of early-age concrete using embedded active acoustic and non-contact complex resistivity methods. Constr. Build. Mater. 2013, 46, 183–192.

31. Pan, H.H.; Huang, M.W. Piezoelectric cement sensor-based electromechanical impedance technique for the strength monitoring of cement mortar. Constr. Build. Mater. 2020, 254, 119307.

32. Qin, L.; Lu, Y.; Li, Z. Embedded Cement-Based Piezoelectric Sensors for Acoustic Emission Detection in Concrete. J. Mater. Civ. Eng. 2010, 22, 1323–1327.

33. Rathod, V.T. A Review of Acoustic Impedance Matching Techniques for Piezoelectric Sensors and Transducers. Sensors 2020, 20, 4051.

34. Li, Z.; Zhang, D.; Wu, K. Cement-Based 0-3 Piezoelectric Composites. J. Am. Ceram. Soc. 2004, 85, 305–313.

35. Newnham, R.E.; Safari, A.; Giniewicz, J.; Fox, B.H. Composite piezoelectric sensors. Ferroelectrics 1984, 60, 15–21.

36. Zhang, F.; Feng, P.; Wang, T.; Chen, J. Mechanical-electric response characteristics of 1-3 cement based piezoelectric composite under impact loading. Constr. Build. Mater. 2019, 228, 116781.

37. Dong, B.; Li, Z. Cement-based piezoelectric ceramic smart composites. Compos. Sci. Technol. 2005, 65, 1363–1371.

38. Wittinanon, T.; Rianyoi, R.; Ngamjarurojana, A.; Chaipanich, A. Effect of polyvinylidene fluoride on the acoustic impedance matching, poling enhancement and piezoelectric properties of 0–3 smart lead-free piezoelectric Portland cement composites. J. Electroceram. 2020, 44, 232–241.

39. Wittinanon, T.; Rianyoi, R.; Chaipanich, A. Effect of polyvinylidene fluoride on the fracture microstructure characteristics and piezoelectric and mechanical properties of 0-3 barium zirconate titanate ceramic-cement composites. J. Eur. Ceram. Soc. 2020, 40, 4886–4893.

40. Lu, Y.; Li, Z. Cement-based piezoelectric sensor for acoustic emission detection in concrete structures. In Earth & Space 2008: Engineering, Science, Construction, and Operations in Challenging Environments; American Society of Civil Engineers (ASCE): Reston, VA, USA, 2008; pp. 1–11.

41. Lotfi, H.; Faiz, B.; Moudden, A. Characterization the acoustic impedance of mortar using ultrasonic technique. J. Civ. Eng. Res. 2013, 3, 46–51.

42. UT-Material Properties Tables-Accoustic Properties for Ceramics, Crystals, Glass, & Minerals-NDT Resource Center. Available online: (accessed on 8 January 2021).

43. Zhang, Y.; Liu, Z.; Zhang, W. Improved output voltage of 0–3 cementitious piezoelectric composites with basalt fibers. Ceram. Int. 2019, 45, 6577–6580.

44. Banerjee, S.; Cook-Chennault, K.A. Influence of aluminium inclusions on dielectric properties of three-phase PZT-cement-aluminium composites. Adv. Cem. Res. 2014, 26, 63–76.

45. Ayub, T.; Khan, S.U.; Memon, F.A. Mechanical characteristics of hardened concrete with different mineral admixtures: A review. Sci. World J. 2014, 2014, 875082.

46. Huang, S.; Chang, J.; Liu, F.; Lu, L.; Ye, Z.; Cheng, X. Poling process and piezoelectric properties of lead zirconate titanate sulphoaluminate cement composites. J. Mater. Sci. 2004, 39, 6975–6979.

47. Chaipanich, A.; Jaitanong, N.; Tunkasiri, T. Fabrication and properties of PZT-ordinary Portland cement composites. Mater. Lett. 2007, 61, 5206–5208.

48. Chaipanich, A. Effect of PZT particle size on dielectric and piezoelectric properties of PZT-cement composites. Curr. Appl. Phys. 2007, 7, 574–577.

49. Pan, H.H.; Chiang, C.-K. Effect of aged binder on piezoelectric properties of cement-based piezoelectric composites. Acta Mech. 2014, 225, 1287–1299.

50. Chomyen, P.; Potong, R.; Rianyoi, R.; Ngamjarurojana, A.; Chindaprasirt, P.; Chaipanich, A. Microstructure, dielectric and piezoelectric properties of 0–3 lead free barium zirconate titanate ceramic-Portland fly ash cement composites. Ceram. Int. 2018, 44, 76–82.

51. Chaipanich, A. Dielectric and piezoelectric properties of PZT-silica fume cement composites. Curr. Appl. Phys. 2007, 7, 532–536.

52. Wang, F.; Wang, H.; Song, Y.; Sun, H. High piezoelectricity 0–3 cement-based piezoelectric composites. Mater. Lett. 2012, 76, 208–210.

53. Pan, H.H.; Yang, R.-H.; Cheng, Y.-C. High piezoelectric properties of cement piezoelectric composites containing kaolin. In Structural Health Monitoring and Inspection of Advanced Materials, Aerospace, and Civil Infrastructure 2015; International Society for Optics and Photonics: San Diego, CA, USA, 2015; Volume 9437.

54. Jaitanong, N.; Wongjinda, K.; Tammakun, P.; Rujijanagul, G.; Chaipanich, A. Effect of Carbon Addition on Dielectric Properties of 0-3 PZT-Portland Cement Composite. Adv. Mater. Res. 2008, 55–57, 377–380.

55. Huang, S.; Li, X.; Liu, F.; Chang, J.; Xu, D.; Cheng, X. Effect of carbon black on properties of 0–3 piezoelectric ceramic/cement composites. Curr. Appl. Phys. 2009, 9, 1191–1194.

56. Gong, H.; Li, Z.; Zhang, Y.; Fan, R. Piezoelectric and dielectric behavior of 0–3 cement-based composites mixed with carbon black. J. Eur. Ceram. Soc. 2009, 29, 2013–2019.

57. Zhao, P.; Wang, S.; Kadlec, A.; Li, Z.; Wang, X. Properties of cement–sand-based piezoelectric composites with carbon nanotubes modification. Ceram. Int. 2016, 42, 15030–15034.

58. Jaitanong, N.; Narksitipan, S.; Ngamjarurojana, A.; Chaipanich, A. Influence of graphene nanoplatelets on morphological and electrical properties of silica fume blended cement—Piezoelectric ceramic composite. Ceram. Int. 2018, 44, S137–S140.

59. Huang, S.; Ye, Z.; Hu, Y.; Chang, J.; Lu, L.; Cheng, X. Effect of forming pressures on electric properties of piezoelectric ceramic/sulphoaluminate cement composites. Compos. Sci. Technol. 2007, 67, 135–139.

60. Pan, H.H.; Wang, C.K.; Cheng, Y.C. Curing time and heating conditions for piezoelectric properties of cement-based composites containing PZT. Constr. Build. Mater. 2016, 129, 140–147.

61. Li, Z.; Dong, B.; Zhang, D. Influence of polarization on properties of 0–3 cement-based PZT composites. Cem. Concr. Compos. 2005, 27, 27–32.

62. Cheng, X.; Huang, S.; Chang, J.; Lu, L.; Liu, F.; Ye, Z.; Wang, S. Dielectric and piezoelectric properties of piezoelectric ceramic–sulphoaluminate cement composites. Smart Mater. Struct. 2005, 14, N59–N63.

63. Chaipanich, A.; Rianyoi, R.; Potong, R.; Jaitanong, N. Aging of 0–3 piezoelectric PZT ceramic–Portland cement composites. Ceram. Int. 2014, 40, 13579–13584.

64. Pan, H.H.; Wang, C.K.; Tia, M.; Su, Y.M. Influence of water-to-cement ratio on piezoelectric properties of cement-based composites containing PZT particles. Constr. Build. Mater. 2020, 239, 117858.

65. Lu, Y.; Zhang, J.; Li, Z.; Dong, B. Corrosion monitoring of reinforced concrete beam using embedded cement-based piezoelectric sensor. Mag. Concr. Res. 2013, 65, 1265–1276.

66. Dong, B.; Xing, F.; Li, Z. Cement-based piezoelectric ceramic composite and its sensor applications in civil engineering. ACI Mater. J. 2011, 108, 543–549.

67. Rianyoi, R.; Potong, R.; Ngamjarurojana, A.; Chaipanich, A. Influence of barium titanate content and particle size on electromechanical coupling coefficient of lead-free piezoelectric ceramic-Portland cement composites. Ceram. Int. 2013, 39, S47–S51.

68. Rianyoi, R.; Potong, R.; Ngamjarurojana, A.; Chaipanich, A. Microstructure and electrical properties of 0–3 connectivity barium titanate−Portland cement composite with 40% barium titanate content. Ferroelectr. Lett. Sect. 2016, 43, 59–64.

69. Rianyoi, R.; Potong, R.; Jaitanong, N.; Yimnirun, R.; Chaipanich, A. Dielectric, ferroelectric and piezoelectric properties of 0–3 barium titanate–Portland cement composites. Appl. Phys. A 2011, 104, 661–666.

70. Potong, R.; Rianyoi, R.; Ngamjarurojana, A.; Yimnirun, R.; Guo, R.; Bhalla, A.S.; Chaipanich, A. Acoustic and Piezoelectric Properties of 0–3 Barium Zirconate Titanate-Portland Cement Composites-Effects of BZT Content and Particle Size. Ferroelectrics 2013, 455, 69–76.

71. Potong, R.; Rianyoi, R.; Ngamjarurojana, A.; Yimnirun, R.; Guo, R.; Bhalla, A.S.; Chaipanich, A. Effect of particle size on dielectric properties and hysteresis behavior of 0–3 barium zirconate titanate-Portland cement composites. Integr. Ferroelectr. 2013, 148, 131–137.

72. Potong, R.; Rianyoi, R.; Ngamjarurojana, A.; Yimnirun, R.; Guo, R.; Bhalla, A.S.; Chaipanich, A. Thermal expansion behaviors of 0–3 connectivity lead-free barium zirconate titanate-Portland cement composites. Ceram. Int. 2017, 43, S129–S135.

73. Potong, R.; Rianyoi, R.; Chaipanich, A. Dielectric properties of lead-free composites from 0–3 barium zirconate titanate-Portland cement composites. Ferroelectr. Lett. Sect. 2011, 38, 18–23.

74. Hunpratub, S.; Yamwong, T.; Srilomsak, S.; Maensiri, S.; Chindaprasirt, P. Effect of particle size on the dielectric and piezoelectric properties of 0–3 BCTZO/cement composites. Ceram. Int. 2014, 40, 1209–1213.

75. Rianyoi, R.; Potong, R.; Ngamjarurojana, A.; Chaipanich, A. Poling effects and piezoelectric properties of PVDF-modified 0–3 connectivity cement-based/lead-free 0.94(Bi0.5Na0.5)TiO3–0.06BaTiO3 piezoelectric ceramic composites. J. Mater. Sci. 2018, 53, 345–355.

76. Potong, R.; Rianyoi, R.; Ngamjarurojana, A.; Chaipanich, A. Influence of carbon nanotubes on the performance of bismuth sodium titanate-bismuth potassium titanate-barium titanate ceramic/cement composites. Ceram. Int. 2017, 43, S75–S78.

77. Santos, J.A.; Sanches, A.O.; Akasaki, J.L.; Tashima, M.M.; Longo, E.; Malmonge, J.A. Influence of PZT insertion on Portland cement curing process and piezoelectric properties of 0–3 cement-based composites by impedance spectroscopy. Constr. Build. Mater. 2020, 238, 117675.

78. Kantakam, S.; Pimraksa, K.; Ngamjarurojana, A.; Chindaprasirt, P.; Chaipanich, A. Investigation on the Dielectric Properties of 0–3 Lead Zirconate Titanate-Geopolymer Composites. Ferroelectrics 2013, 451, 84–89.

79. Pan, H.H.; Lin, D.-H.; Yang, R.-H. High piezoelectric and dielectric properties of 0–3 PZT/cement composites by temperature treatment. Cem. Concr. Compos. 2016, 72, 1–8.

80. Chen, J.; Qiu, Q.; Han, Y.; Lau, D. Piezoelectric materials for sustainable building structures: Fundamentals and applications. Renew. Sustain. Energy Rev. 2019, 101, 14–25.

81. Jaitanong, N.; Chaipanich, A.; Tunkasiri, T. Properties 0–3 PZT–Portland cement composites. Ceram. Int. 2008, 34, 793–795.

82. Gong, H.; Zhang, Y.; Quan, J.; Che, S. Preparation and properties of cement based piezoelectric composites modified by CNTs. Curr. Appl. Phys. 2011, 11, 653–656.

83. Huang, S.; Lu, L.; Chang, J.; Xu, D.; Liu, F.; Cheng, X. Influence of ceramic particle size on piezoelectric properties of cement-based piezoelectric composites. Ferroelectrics 2006, 332, 187–194.